J Stat Phys (2009) 135: 991–1008
DOI 10.1007/s10955-009-9710-8

Phase Coexistence in Nanoscopically Thin Films Confined by Asymmetric Walls

Ezequiel V. Albano · Kurt Binder

Received: 25 February 2009 / Accepted: 27 February 2009 / Published online: 21 March 2009

Abstract Thin Ising films with nearest-neighbor ferromagnetic exchange in a bulk magnetic field H are studied in a $L \times L \times D$ geometry, where at the opposite walls, given by the $L \times L$ surfaces, local magnetic fields H_1, and H_D act. While in previous work, the symmetric case $H_1 = H_D$ (leading to "capillary condensation", when one applies the lattice gas terminology) as well as the antisymmetric case $H_1 = -H_D$ (leading to "interface localization transitions") were studied, we focus here on the general 'asymmetric' case. Monte Carlo simulations are carried out and analyses based on thermodynamic integration methods are used to establish the phase diagrams and study the properties of the coexisting phases. A discussion is given why for the range of thicknesses that is explored ($16 \leq D \leq 80$ lattice spacings) this is the most suitable methodology. Restricting attention to cases where in the semi-infinite system a first-order wetting transition occurs, it is shown that the latter, due to confinement, is turned in a thin-film triple point. Above the triple point, narrow two-phase coexistence curves are found, which are the analog of prewetting transitions in the semi-infinite system. A comparison to related results for (symmetrical) polymer blends and (asymmetric) colloid-polymer mixtures is made.

Keywords Interface localization · Wetting · Ising model · Monte Carlo simulation · Capillary condensation

1 Introduction

When systems capable to undergo phase transitions (e.g. ferro- and antiferro-magnets that may undergo a transition to the paramagnetic phase, solid or fluid binary mixtures that may

E.V. Albano
Instituto de Investigaciones Fisicoquímicas Teóricas y Aplicadas (INIFTA), CCT La Plata, CONICET, UNLP, Casilla de Correo 16, Sucursal 4, 1900 La Plata, Argentina

K. Binder (✉)
Institut für Physik, Johannes Gutenberg Universität, Staudinger Weg 7, 55099 Mainz, Germany
e-mail: kurt.binder@uni-mainz.de

undergo phase separation, simple fluids that may undergo the liquid-vapor transition, etc.) are confined in a thin film geometry, their phase behavior is strongly modified through a combination of finite-size effects (due to the finite thickness D of the thin film) and surface effects (caused by the confining walls) [1–27]. In the bulk, a generic and convenient model to study these phase transitions has been the Ising model [28, 29]; hence, it is plausible that much of the theoretical work devoted to study confinement effects on phase transitions has relied on Ising model studies as well ([1, 2, 4–6, 10–13, 19, 20, 23] give a selection of the literature on this subject). However, all of this work has invoked special symmetries with respect to the boundaries, in addition to the spin up/spin down symmetry (or equivalently, particle-hole symmetry in the lattice gas interpretation of the Ising model [29]) that is present in the bulk: normally, the case of a thin film confined by two equivalent walls is considered [1, 2, 4, 6, 10, 19, 20]. Assuming that one of the spin up/spin down phases coexisting in the bulk at zero bulk magnetic field, $H = 0$, is preferred by the walls, it is natural to introduce at the walls "surface magnetic fields" ($H_1 = H_D$) that act on the spins in the respective surface planes only [30, 31]. The resulting shift of phase coexistence from $H = 0$ in the bulk to a value $H_{coex}(H_1, D, T) \neq 0$ is the analog of "capillary condensation or evaporation" in fluids [7, 14] (note that in a simple cubic or square lattice, one simply has $H_{coex}(H_1, D, T) = -2H_1/D$ when the temperature T tends to zero [1, 2]).

Only more recently [5, 8, 9, 11–13, 23], also the case of antisymmetric walls $H_1 = -H_D$ (also called "competing walls") has found increasing attention. Then, phase coexistence again occurs for $H = 0$, but in addition to this transition from a (predominantly) "spin up"-phase to a "spin down"-phase, one encounters the "interface localization transition" [8, 9, 20]: while the interface between these phases at low temperature is tightly bound to one of the walls, at higher temperatures the interface is unbound from the walls, freely fluctuating in the center of the thin film ("softmode phase" [9]).

Of course, when experiments are done, it is unlikely that such a special symmetry of confining walls can be realized [20, 27]. E.g., one can prepare mixtures of two polymers that have in the bulk an almost symmetric phase diagram, and if one brings a thin film on a substrate and studies the interface between the two coexisting phases, some signatures of the "soft mode phase" can be observed [32, 33]. Clearly, there is no special "antisymmetry" between the lower substrate-polymer surface and the upper polymer-air surface of such a film. It is to be expected that such nanoscopically thin two-or more-component thin films, that show phase separation and form an interface parallel to the substrate, will find interesting applications in nanotechnology [34–36].

The present paper thus attempts to close this gap by presenting the first Monte Carlo simulation of an Ising ferromagnet confined between walls with surface magnetic fields H_1, H_D that lack any particular symmetry. A related problem has only been considered within the (mean-field type) self-consistent field method for a polymer blend [17]. Asymmetry effects were also treated for confined colloid-polymer mixtures [26, 27], but there the phase diagram is already very asymmetric in the bulk, in the absence of boundaries.

The plan of this paper is as follows: In Sect. 2, we introduce the model and define the quantities that are calculated. Section 3 gives a discussion of the methodology of simulation and "data" analysis that we find efficient for this problem. Section 4 then presents our results, while Sect. 5 gives a discussion and a speculative extension of the developed concepts to describe the possible phase diagrams for other cases than those that were simulated.

2 The Ising Film with Competing Surface Fields

We consider the nearest-neighbor Ising ferromagnet on the simple cubic lattice, choosing a $L \times L \times D$ geometry with two free surface layers of size $L \times L$ at layers $n = 1$ and $n = D$ (taking the lattice spacing as our unit of length). Periodic boundary conditions are applied in both x- and y-directions. The Hamiltonian $\mathcal{H}$ of the system then is given by

$$\mathcal{H} = -J \sum_{\langle i,j\rangle \text{bulk}} S_i S_j - J_s \sum_{\langle i,j\rangle \text{both from the surfaces}} S_i S_j - H \sum_i S_i$$
$$- H_1 \sum_{i \in n=1} S_i - H_D \sum_{i \in n=D} S_i, \quad S_i = \pm 1. \tag{1}$$

The first sum runs over all nearest-neighbor pairs of spins where at least one spin is not in the surface planes $n = 1$ or $n = D$, respectively. Following [37–39], we allow for an exchange coupling $J_s (> 0)$ in the surface planes different from the exchange constant J in the bulk ($J > 0$ as well). The second sum runs over those spins where both sites i, j are from the surface planes $n = 1$ or $n = D$, respectively. The reason why $J_s > J$ is of interest is that only then the possibility arises that in semi-infinite geometry wetting transitions [40–43] of first-order occur (while for $J_s = J$, one always finds second-order wetting transitions, i.e. "critical wetting", in this model [37, 38]). While critical wetting with short range forces is of particular theoretical interest [44, 45], it is delicate to observe critical wetting experimentally [43]; and since for $D \to \infty$, the interface localization transition (for the antisymmetric case $H_1 = -H_D$) reduces to the wetting transition, it is of greater practical relevance to study cases where then first-order wetting occurs. The third sum in (1) describes the Zeeman energy gain due to a bulk magnetic field, while the last two sums describe the coupling to the surface magnetic fields H_1, H_D (remember that in the lattice gas interpretation, these terms transform into some local binding potential, acting from the confining walls on the particles; see e.g. [10] for a discussion).

The Ising ferromagnet in the bulk in $d = 3$ dimensions and in the absence of a magnetic field undergoes a second-order phase transition from the ferromagnetic to the paramagnetic phase, at the bulk critical temperature $k_B T_{cb}/J = 4.51142 \pm 0.00005$ [46]. In the following, temperatures are reported in units of J and we put $k_B \equiv 1$.

We now redefine the index "i" of a lattice site by its actual coordinates (j, k, n) where j represents the x-coordinate of the site, k the y-coordinate, and n the z-coordinate (or layer index, which runs from $n = 1$ to $n = D$). A useful quantity then is the average magnetization in the nth layer,

$$m_n = \langle \tilde{M}(n) \rangle \equiv \left\langle \frac{1}{L^2} \sum_{j=1}^{L} \sum_{k=1}^{L} S(j,k,n) \right\rangle. \tag{2}$$

The thermal average $\langle \ldots \rangle$ is computed by straightforward Monte Carlo sampling applying the Metropolis algorithm [47] (see Sect. 3 for a discussion of the choice of algorithms). Of course, the total magnetization is simply an average of m_n over all the layers, again normalized per spin

$$m_{av} = (1/D) \sum_{n=1}^{D} m_n. \tag{3}$$

Finally, we note that the average energy per spin simply is

$$U = [L^2 D]^{-1} \langle \mathcal{H} \rangle. \tag{4}$$

As discussed in [37–39], in the context of critical wetting phenomena, it is of interest to study also various layer susceptibilities χ_n and χ_{nn}. Being primarily interested in a study of phase transitions that are strongly of first-order, however, the behavior of these susceptibilities is less interesting, and hence will not be discussed here. For the choice $J_s/J = 1.4$, which is used in the present paper throughout, the wetting transition is strongly first-order [37, 38].

3 Methodology of Simulation and "Data" Analysis

When one simulates Ising systems, the first choice to be made corresponds to the simulation algorithm. Dealing with critical phenomena in the bulk in the absence of any magnetic fields, the use of the Swendsen-Wang [47, 48] or Wolff [47, 49] cluster algorithm would be the method of choice. However, a study of capillary condensation in thin Ising films near the bulk critical point [19] has shown that such algorithms are efficient only for extremely small surface fields, and hence not suitable in the present context.

Another presently very popular algorithm, Wang-Landau sampling [50, 51], has been successfully applied [23] for the study of interface localization transitions in the case of strictly antisymmetric surface fields. However, it turned out that in the case of first-order transitions, the accuracy of the method is problematic due to [23] the presence of "entropic barriers" as discussed in [52].

Since it is clear that for interface localization transitions that are strongly first-order, the application of finite-size scaling methods [53–56] has little advantage [13], we conclude that the best way to proceed is to simulate very large systems with the straightforward Metropolis Algorithm [47] and locate first-order transitions by equating the free energies of the appropriate phases. These free energies in turn can be accurately obtained by thermodynamic integration [47, 57].

Since in the limit of very thick films ($D \to \infty$), interface localization transitions are predicted to converge towards wetting transitions [8, 9, 20], we first discuss how the location of the first-order wetting transitions can be estimated. We note that the free energy of the model (1), for large D, can be decomposed as [30, 31, 58]

$$f(T, H, H_1, H_D, D) = f_b(T, H) + \frac{1}{D} f_s(T, H, H_1) + \frac{1}{D} f_s(T, H, H_D). \tag{5}$$

Here, $f_b(T, H)$ is the free energy (per spin) of a bulk Ising system, which depends on neither H_1 nor H_D, of course. $f_s(T, H, H_1)$ is the surface excess free energy of the left wall, where the field H_1 acts, while $f_s(T, H, H_D)$ refers to the surface excess free energy of the right wall where H_D acts. Of course, (5) holds only in the limit of very thick films where the interaction between wetting layers associated with both walls can be neglected. Wetting transitions show up as singularities of the respective surface excess free energies [20, 40–43].

Assuming now $H_1 < 0$, a wetting transition occurs at the left surface when $H \to 0^+$, so we have a positive spontaneous magnetization $m_b(T, H = 0^+)$

$$m_b = -(\partial f_b(T, H)/\partial H)_T \tag{6}$$

in the bulk. In the non-wet phase, $f_s^{(+)}(T, 0, H_1)$ then is the excess free energy of a surface where the region of positive magnetization in the film extends close to the left wall. In the

wet phase, however, we have a (macroscopically thick) domain of the negative magnetization adjacent to the left wall, separated by an interface (i.e. a domain wall of the same type as between coexisting oppositely oriented domains in the bulk) from the domain with positive magnetization which takes the bulk of the film. Consequently, the surface excess free energy of a wet surface is

$$f_s^{\rm wet}(T,0,H_1) = f_s^{(-)}(T,0,H_1) + f_{int}(T,0). \tag{7}$$

Here, $f_s^{(-)}(T,0,H_1)$ is the excess free energy of a surface where both the bulk magnetization and the surface field H_1 are negative, and $f_{int}(T,0)$ is the interfacial free energy of the Ising model (which is rather accurately known due to previous work [59, 60]). So, the wetting transition occurs when

$$f_s^{(+)}(T,0,H_1) = f_s^{(-)}(T,0,H_1) + f_{int}(T,0). \tag{8}$$

Note that (8) can be also derived by using Young's equation for the contact angle Θ

$$f_{int}(T,0)\cos\Theta = f_s^{(+)}(T,0,H_1) - f_s^{(-)}(T,0,H_1) \tag{9}$$

and putting $\Theta = 0$ [40–43], of course.

In the Ising ferromagnet, it is convenient to make use of the symmetry relation

$$f_s^{(-)}(T,0,H_1) = f_s^{(+)}(T,0,-H_1), \tag{10}$$

where $f_s^{(+)}(T,0,-H_1)$ is the excess free energy of a surface where the region of positive magnetization in the film extends to a wall where a positive surface field $(-H_1)$ acts. Using a film with a boundary condition of antisymmetric fields, $H_D = -H_1$, we further conclude

$$f_s^{(-)}(T,0,-H_1) = f_s^{(+)}(T,0,H_D), \tag{11}$$

and hence the relevant free energy difference needed to locate the wetting transition simply becomes $\Delta f_{1D} \equiv f_s^{(+)}(T,0,H_1) - f_s^{(+)}(T,0,H_D)$. Using now the relations [30, 31, 58]

$$m_1 = -(\partial f_s(T,H,H_1)/\partial H_1)_T, \qquad m_D = -(f_s(T,H,H_D)/\partial H_D)_T, \tag{12}$$

we find

$$\Delta f_{1D} = f_s^{(+)}(T,0,H_1) - f_s^{(+)}(T,0,H_D) = \int_0^{H_1} (m_D - m_1)\, dH_1', \tag{13}$$

performing a calculation where the surface fields $H_1' < 0$, $H_D' = -H_1' > 0$ are varied for a film with positive magnetization. This method for the location of a first-order wetting transition has previously been used successfully in the case of symmetric polymer mixtures [61].

In practice, we start at $H_D = -H_1 = 0$ with a system of size $L = D = 64$ by taking an ordered initial configuration with $s(j,k,n) = +1$, all spins pointing up. At the temperature chosen, $T = 4$, which is about 10 percent lower than the critical temperature of the bulk, $T_{cb} = 4.51142 \pm 0.00005$ [46], it suffices to average over 3×10^4 Monte Carlo steps per site (MCS), after discarding the first 2×10^4 MCS. Figure 1 plots the results for Δf_{1D} as a function of H_1. In practice, we have found that (13) can be discretized in steps of $\Delta H_1 = 0.0125$ to make the numerical integration error small enough for our purposes (note that fields are quoted in units of J as well). The intersection with $f_{int}(T = 4.0)$ taken from [59, 60] yields the field at which the wetting transition occurs as $H_1^{\rm wet} = 0.3180$ (5).

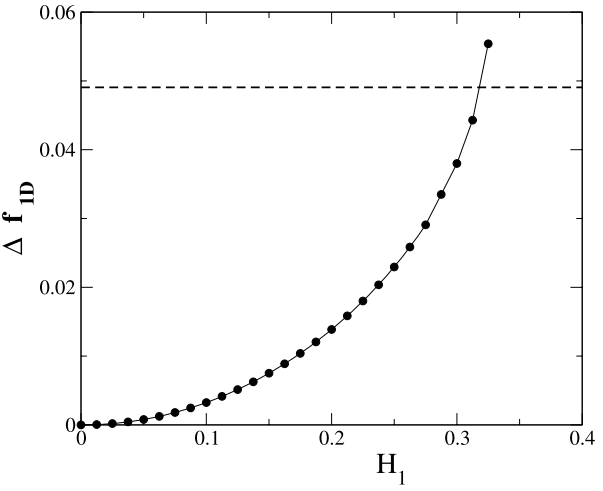

Fig. 1 Plot of Δf_{1D} (Eq. (13)) versus H_1, for the case $H = 0$, $J_s/J = 1.4$, $T = 4$. The (*horizontal*) *dashed line* corresponds to the interfacial free energy of the Ising ferromagnet at the same temperature, as reported by Hasenbusch and Pinn [59, 60]

Near the wetting transition, we have further enlarged the system choosing $L = D = 128$, in order to make sure that finite-size effects play no role. The fact that the curve for $\Delta f_{1D}(H_1)$ intersects $f_{int}(T, 0)$ in Fig. 1 at a large angle is a clear indication that the wetting transition is strongly of first order, however, and hence it is not surprising that no significant finite-size effects occur.

When H_D differs from $-H_1$, and finite values of D are considered, phase transitions of the thin film occur in general at $H \neq 0$, and in order to locate them, we also use thermodynamic integration methods, by using now an equation analogous to (6),

$$m_{av} = -(\partial f(T, H, H_1, H_D, D)/\partial H)_{T,H_1,H_D}, \tag{14}$$

to conclude

$$\Delta f = f_2 - f_1 = -\int_{H^{(1)}}^{H^{(2)}} m_{av} dH', \tag{15}$$

for the free energy difference between two states where the bulk magnetic field is varied from $H^{(1)}$ to $H^{(2)}$ and the system does not perform a phase transition along this path. While in the case of (13) due to the symmetry of the problem, no reference state with known free energy was needed, this is no longer the case here, however. We thus use here reference states at very low temperature, using the relation for the internal energy u per spin

$$u = (\partial f/\partial\beta)_{H,H_1,H_D}, \quad \beta = 1/T, \tag{16}$$

so that [47, 57]

$$\beta f(\beta) = \beta_0 f(\beta_0) + \int_{\beta_0}^{\beta} u(\beta')d\beta'. \tag{17}$$

Since we are interested at $T < T_{cb}$, using the reference state of infinite temperature ($\beta_0 = 0$) is not convenient, and we rather wish to use $T = 0$ as a reference state, where the reference free energy $f(\beta_0)$ is trivially known (since the entropy is zero). However, for the thermodynamic integration, (17), a very large integration interval needs to be avoided,

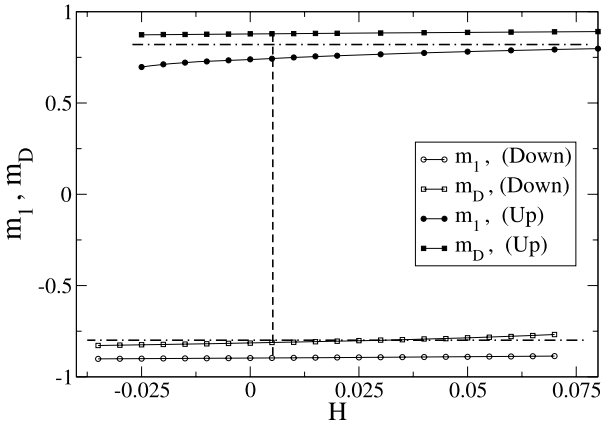

Fig. 2 Plot of the layer magnetization m_1, m_D adjacent to the walls versus the bulk magnetic field, as obtained for $T = 3.8$, surface fields $H_D = -H_1/2$, $H_1 = -0.318$, for lattices of size $D = L = 80$, and using different initial conditions, namely starting from fully ordered configurations with all spins down or all spins up, as indicated in the figure. The *vertical* (*dashed*) *line* shows the location of the transition, as determined by thermodynamic integration methods (see Fig. 3). The (*horizontal*) *dash-dotted lines* indicate the value of the positive and negative spontaneous bulk magnetization for $H = 0$. The *solid curves* connecting the actual simulation "data" points have been drawn to guide the eye

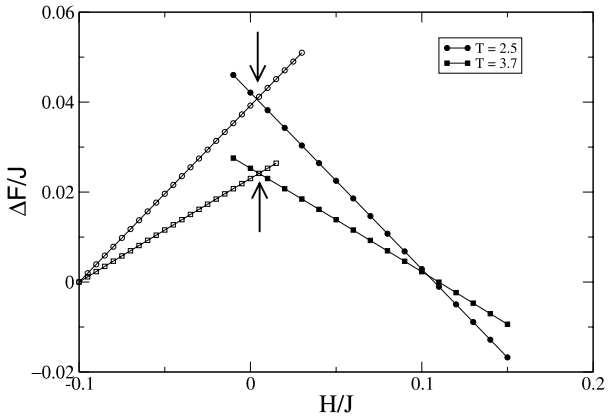

Fig. 3 Estimation of the critical fields where first order transitions of the thin film occur for $H_D = -H_1/2$ and $H_1 = -0.318$, from the intersection of free energy differences (relative to the state at $H/J = 0.1$) between bulk states in different phases. *Open* and full *circles* (*squares*) correspond to results calculated at $T = 2.5$ ($T = 3.7$) and were obtained by starting the simulations with fully ordered configurations with all spins up or all spins down, respectively. Lattices of size $D = L = 80$ were used. The *arrows* show the located critical fields

of course, and hence $\beta_0 \to \infty$ cannot be used. It turns out, however, that $\beta_0 = 0.85$ already is large enough to neglect the entropy.

Figure 2 shows that for the chosen model strong hysteresis occurs, as expected. For temperatures T substantially lower than the wetting transition temperature $T_W(H_1)$, which in our case is $T_W(H_1) = 4.0$, we expect a single transition in the film, but due to the surface fields H_1, H_D it no longer occurs at the bulk field $H = 0$, but at a nontrivial critical value H_c

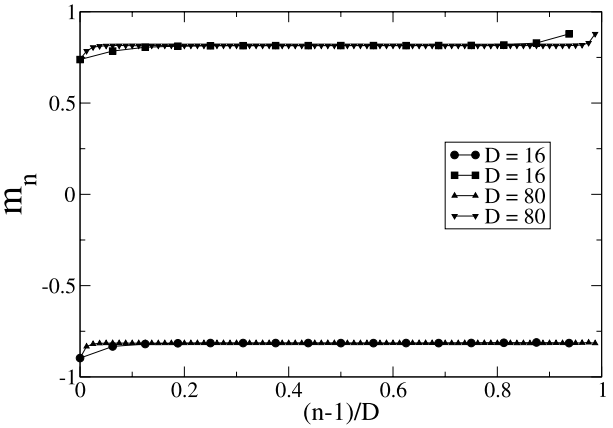

Fig. 4 Plot of the magnetization profile m_n versus the rescaled row distance $(n-1)/D$ obtained at $T = 3.8$ and for films of thickness $D = 16$ and $D = 80$, as indicated. *Upper curves* show results obtained from starting configurations with all spins up, *lower curves* show results obtained from starting configurations will all spins down. *Solid curves* are guides to the eye only. $H = 0$ is chosen throughout

different from zero, analoguous to the case of capillary condensation [1, 2, 10]. Similarly, as for Monte Carlo studies of capillary condensation [10], the critical field can be accurately estimated from intersections of the respective branches of free energy differences, however (Fig. 3). Again, relatively short runs suffice to obtain accurate "raw Monte Carlo data": typically, averages are taken over 8×10^3 MCS after discarding the first 2×10^3 MCS.

4 Results

Two lattice sizes were extensively studied, $L \times L \times D = 80 \times 80 \times 16$ and $80 \times 80 \times 80$, respectively. We first focus on the behavior of the magnetization profiles across the film at different temperatures.

Figure 4 plots m_n vs. the rescaled row distance for two lattice sizes at $T = 3.8$, i.e. at a temperature where (in the limit of large D) both surfaces clearly are nonwet. One sees that in this case, the two competing phases of the film differ only marginally from their homogeneous bulk counterparts; only near the walls, the layer magnetization m_1, m_D differ slightly from $\pm m_b$. Note also neither m_1 nor m_D depend significantly on D.

When we increase the temperature, we reach a regime where (for $D \to \infty$) $T_W(H_1) < T < T_W(H_D)$: since $H_D = -H_1/2$, the wetting transition (for a thin film with negative magnetization in the bulk) for the right surface ($n = D$) of the film occurs at a higher temperature. This regime is realized e.g. for $T = 4.1$ (Fig. 5(a)). One now finds that the two surfaces have a very different effect on the ordering of the thin film: while a small positive magnetic film does stabilize a positive domain on the right hand side of the film, a domain with negative magnetization near the "wet" surface ($i = 1$) is nevertheless present. Changing H shifts the average position of the interface between these domains. The other phase, where m_n is negative throughout the film, does not show a significant enhancement of m_n, even for $n = D$, irrespective of the fact that a positive surface field is acting there. On the other hand, by keeping the bulk field constant ($H = 0.004$ in Fig. 5(b)) but increasing the temperature one observes an abrupt transition of the magnetization profile that is negative throughout the film for low temperatures ($T \leq 4.22$), but at $T = 4.23$ changes due to the development of a positive domain on the right hand side of the film. This transition would become a first-order prewetting transition of the right wall in the thermodynamic limit.

Still, a very different behavior occurs for temperatures falling in the interval $T_W(H_D) < T < T_{cb}$. Choosing $D = 16$ and $H = 0$, one finds that the resulting profile (which almost

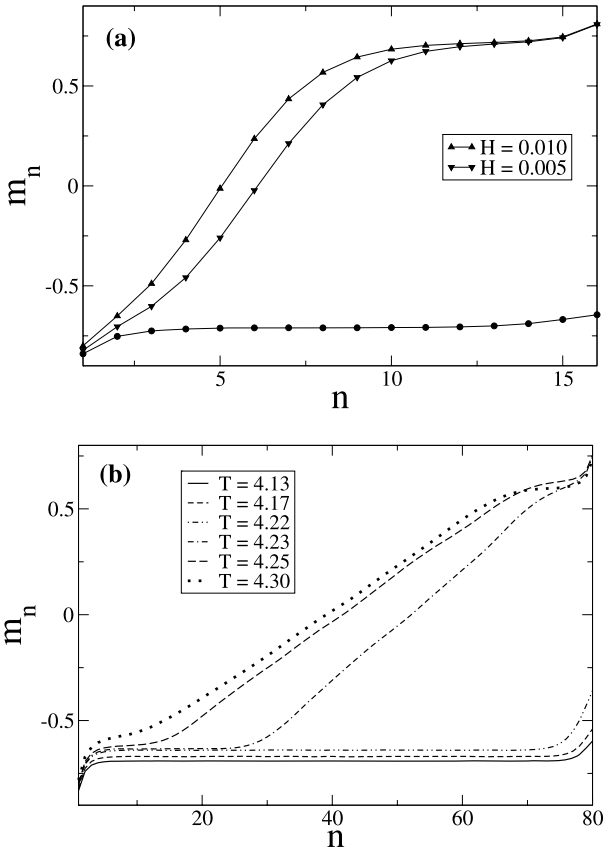

Fig. 5 (**a**) Plot of the magnetization profile m_n versus the row index n as obtained for $T = 4.1$ and for lattices of size $L = 80$, $D = 16$. The *lower curve* was obtained for a starting configuration with all spins down, and $H = 0$, while the *two upper curves* were obtained starting with all spins up and choosing $H > 0$, as indicated. (**b**) Plot of the magnetization profile versus the row index n as obtained for $H = 0.004$ and lattice sizes $L = D = 80$ and various temperatures, as indicated. Note that in between $T = 4.22$ and $T = 4.23$ a transition occurs, which in the thermodynamic limit would become a 1st order prewetting transition of the right wall

satisfies the antisymmetry property, $m_n = -m_{D+1-n}$, that one finds in the case $H_D = -H_1$ [11, 12]) is independent of whether one starts with a state where all spins are up or all spins are down. This lack of hysteresis, as well as the fact that the profile varies almost linearly across the film, are strong indications that the chosen temperature $T = 4.3$ in Fig. 6 exceeds the (maximum) critical temperature $T_c^{(\ell)}(D)$ of the thin film for $D = 16$. This critical temperature $T_c^{(\ell)}(D)$ is the finite thickness analog of the prewetting critical temperature $T_{c,pre}^{(\ell)}$ of the left wall, that is present for a first-order wetting transition, in the limit of a semi-infinite system ($D \to \infty$). In fact, one expects that $T_c^{(\ell)}$ $(D \to \infty) \to T_{c,pre}^{(\ell)}$, while the bulk transition for $H_D = -H_1$ is rounded off [15, 16], and for $H_D = -H_1/2$, the behavior is expected to still resemble the fully antisymmetric case.

It is interesting to note that for a thick film ($D = 80$) at $T = 4.3$, the situation is rather different: by choosing an initial condition "all spins down" at $H = 0$ (which is equivalent to taking the limit $H \to 0^-$) yields a profile that differs significantly from the result obtained for the initial condition "all spins up" at $H = 0$ (which is equivalent to taking the

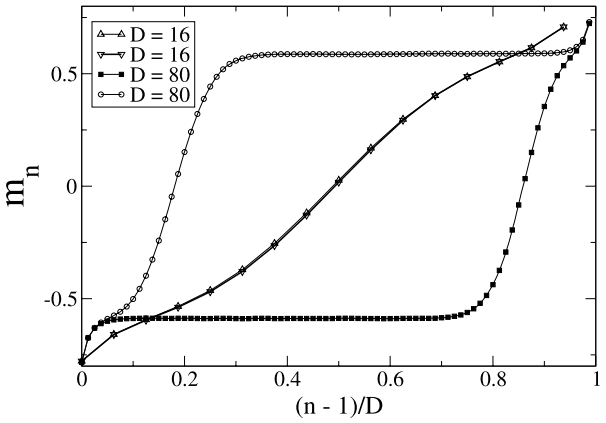

Fig. 6 Plot of the magnetization profile m_n versus the rescaled row index $(n-1)/D$ as obtained at $T = 4.3$ and $H = 0$, for two different film thicknesses, as indicated in the figure. For $D = 80$ the *lower* and the *upper curves* were obtained by starting from fully ordered spin down and spin up-configurations, respectively. For $D = 16$, the same two starting configurations (all spins up or all spins down, respectively) were used, but the results perfectly coincide

limit $H \to 0^+$). This breaking of symmetry caused by these two different initial conditions implies that for $D = 80$, the temperature $T = 4.3$ in fact is lower than $T_c^{(\ell)}(D)$, unlike the case $D = 16$.

For the antisymmetric case $H_D = -H_1$ at $H = 0$, the broken symmetry states with positive and negative total magnetization $(+, -)$ of the thin film satisfy the symmetry

$$m_n^{(+)} = -m_{D+1-n}^{(-)}. \tag{18}$$

Figure 6 shows that (18) is a reasonable approximation still, for the case $H_D = -H_1/2$ considered here.

We also note that the pronounced hysteresis evident from Fig. 2 at low temperatures (such as $T = 3.8$) does not occur when one considers the variation at higher temperatures, e.g. $T = 4.13$ (Fig. 7). One sees that at the right surface a rather pronounced first-order transition occurs at $H_c^{(r)} \approx 0.01$, while the transition at the left surface requires a much stronger field, $H_c^{(\ell)} \approx 0.03$, and is either a weak first-order transition or a second-order transition. This behavior can be understood from the qualitative phase diagrams sketched in Fig. 8: For $D \to \infty$ and $T < T_W^{(\ell)}$, only the bulk transition (from negative to positive magnetization of the whole film, indicated by the double arrows) occurs at $H = 0$. For finite D, this transition occurs now at a field $H_c(T) > 0$, for $T < T_{trip}(D)$, a thin-film triple point. A triple point must occur in the thin film, since in the phase diagram in the (T, H) plane three distinct lines of first order transitions meet: the line $H_c(T)$ is the analog of the transition between "spin down" and "spin up"-phases in the bulk, while the two other lines will be explained in the following. For $T > T_{trip}(D)$, there exists a first-order transition line from $T_{trip}(D)$ to $T_c^{(\ell)}(D)$, which is the analog of the prewetting line from $T_W^{(\ell)}$ to $T_{c,pre}^{(\ell)}$ in the limit $D \to \infty$. Note that no wetting transition is possible for $D < \infty$, since no macroscopically thick wetting layer would fit into a thin film, and so the character of the transition changes from a singularity of the surface excess free energy (for $D \to \infty$ at $T_W^{(\ell)}$) to a singularity of the total film free energy (for finite D at $T_{trip}^{(D)}$ and $H_{trip}(D)$).

Since for finite D the transition line at $T_W^{(r)} < T < T_{cb}$ at $H = 0$ is rounded off, the singularity at $H = 0$, $T_W^{(r)}$ is rounded off as well, and the two transition lines (from $T_W^{(\ell)}$ to $T_W^{(r)}$ at $H = 0$, and from $T_W^{(r)}$ to $T_{c,pre}^{(r)}$) that exist separately for $D \to \infty$ become part of one smooth transition line from $T_{trip}^{(D)}$ to $T_c^{(r)}(D)$ for finite D. The thin film critical point $T_c^{(r)}(D)$ smoothly merges into $T_{c,pre}^{(r)}$ as $D \to \infty$, of course, only the line from $T_W^{(r)}$ to T_{cb} at

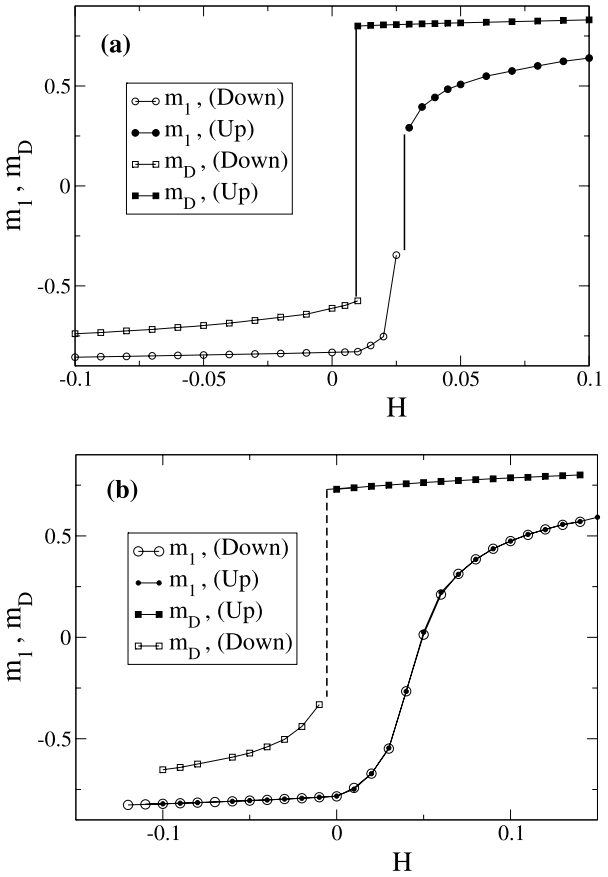

Fig. 7 Plot of the magnetization of the layers adjacent to the walls versus the bulk magnetic field, as obtained for $T = 4.13$, choosing $D = L = 80$, and using different initial conditions, namely "all spins down" or "all spins up", as indicated in the figure. The *vertical straight lines* show the approximate location of the transitions. The *solid lines* linking the data points have only been drawn to guide the eye. (**b**) Same as (**a**), but for $T = 4.3$

$H = 0$ appears in this limit discontinuously. Thus, on the basis of Fig. 8, it is clear that there exists a temperature regime, namely $T_{trip}(D) < T < T_c^{(\ell)}(D)$, where scanning the magnetic field we encounter two transitions: at smaller fields, when the line from $T_{trip}(D)$ to $T_c^{(r)}(D)$ is crossed, at the right surface, the positive surface field "wins" to stabilize a domain with positive magnetization adjacent to this surface, separated by an interface from a domain with negative magnetization at the left wall. A larger value of the field is then needed (crossing the line from $T_{trip}(D)$ to $T_c^{(\ell)}(D)$) to overcome the (stronger) negative surface field at the left wall, and overturn this domain with negative magnetization in the thin film.

This is the situation encountered in Fig. 7a. For $T_c^{(\ell)}(D) < T < T_c^{(r)}(D)$, however, a single transition on the right side of the film is observed, Fig. 7b, while the variation of the magnetization at the left side of the thin film is a smooth crossover, no longer involving any transition. Enhancing the temperature further (Fig. 9), the jump of m_D gets smaller and disappears, when $T_c^{(r)}\ (D)$ is crossed, and for $T > T_c^{(r)}\ (D)$, the variation of the magnetic field only causes a smooth transition from a film with negative magnetization to a film with

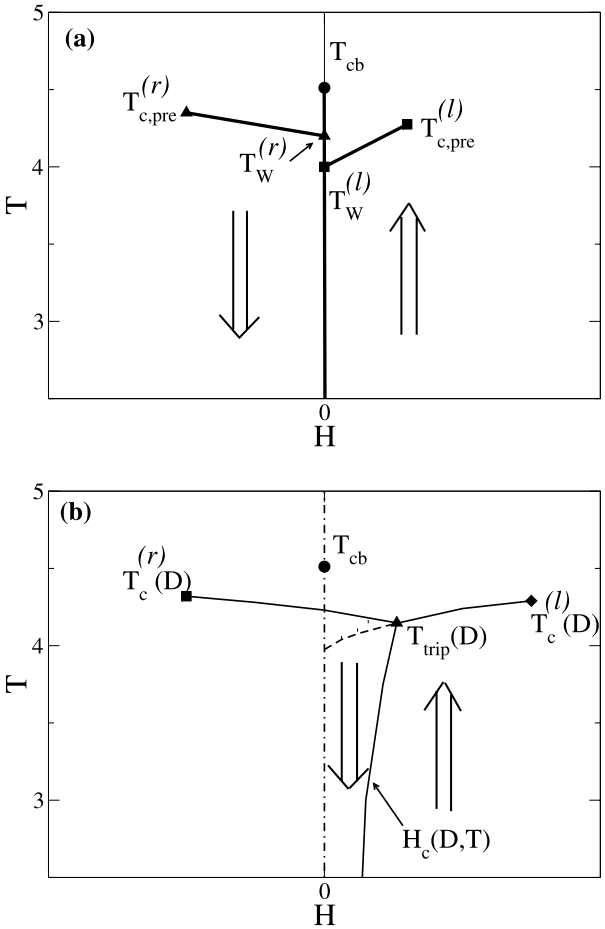

Fig. 8 Schematic phase diagram of a system with surface fields H_1, H_D of opposite sign and different strength ($H_D < |H_1|$, H_1 is chosen negative), in the limit $D \to \infty$ (**a**) and for a film of finite thickness (**b**). Note that the interface roughening transition and its possible complications for the wetting and interface localization phase diagrams are disregarded here

positive magnetization, by gradual unbinding of the interface from the left wall and its motion to the right wall, but this does not cause a transition with a thermodynamic singularity any longer.

The transitions discussed via Figs. 7–9 also show up when one studies the temperature dependence of the layer magnetization (Fig. 10). In principle, one should study the phase diagram along two paths $H \to H_c^-(D,T)$, $H \to H_c^+(D,T)$, approaching the first order transition line in the lower part of Fig. 8 from both sides. Since our estimation of $H_c(D,T)$ suffers from some statistical and systematic errors (finite-size effects, errors in the numerical integrations needed to estimate free energy differences, etc.), we rather followed two paths at $H = 0$, choosing different initial conditions (for $H = 0$, the phase with positive magnetization is still metastable). In this way, Fig. 10 does not yield an estimate for $T_{trip}(D)$, of course, rather one gets enough estimates of $T_W^{(\ell)}$ (when the curve from $T_c^{(\ell)}(D)$ to $T_{trip}(D)$

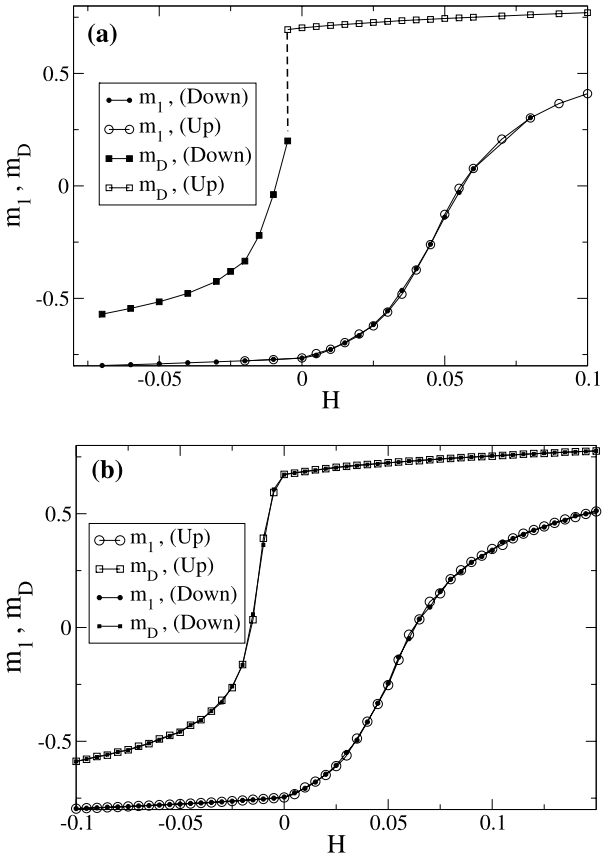

Fig. 9 Layer magnetization m_1, m_D plotted versus magnetic field for $D = L = 80$ and $T = 4.35$ (**a**) and $T = 4.40$ (**b**), using different initial conditions ("all spins down", "all spins up"), as indicated. The *vertical broken line* in (**a**) indicates the first order transition associated with the crossing of the line from $T_{trip}(D)$ to $T_c^{(r)}(D)$ in Fig. 8. Note that no singular behavior related to $T_W^{(r)}$ is left for finite D^c: one can only expect that the line from $T_{trip}(D)$ to $T_c^{(r)}(D)$ has a rounded kink near $T_W^{(r)}$

is continued as a metastable branch towards $H = 0$) and of the transition point where the line from $T_{trip}(D)$ to $T_c^{(r)}(D)$ crosses the $H = 0$ axis (see Fig. 8, lower part).

5 Phase Diagrams

The results for the phase boundary of the "main" transition where the total magnetization of the thin film changes sign are collected in Fig. 11, showing data for two film thicknesses ($D = 16$ and $D = 80$, respectively). It is seen that $H_c(D, T)$ is always positive, for the cases that were investigated, and increases with temperature until about $T_{trip}(D)$, with $T_{trip}(D) \approx 4.0 \pm 0.1$ within our limited accuracy being indistinguishable from $T_W^{(\ell)}$. The transition line from $T_{trip}(D)$ to $T_c^{(\ell)}(D)$ has not been included in Fig. 11 in order to avoid making this figure too confusing, and is deferred to Fig. 12 below. On general grounds, we expect that

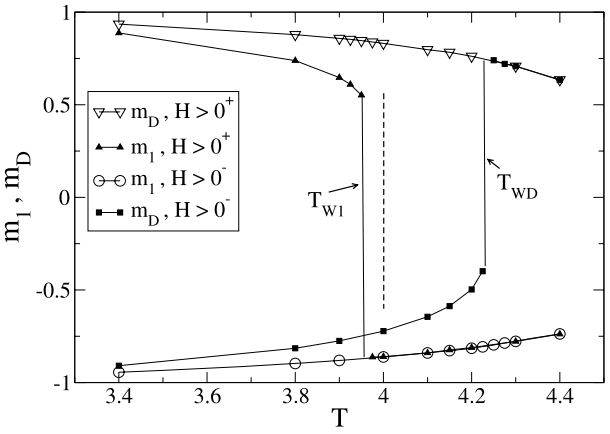

Fig. 10 Layer magnetization m_1, m_D plotted vs. temperature for the case $D = L = 80$ and zero magnetic field, using different initial conditions ("all spins up", "all spins down", as indicated). *Vertical broken lines* denoted as T_{W1}, T_{WD} show the location of the "effective" wetting transitions (these results are presumably strongly affected by finite size effects; for the chosen value $H_1 = -0.318$ of the surface magnetic field, we rather expect the wetting transition temperature at $T_W^{(\ell)} = 4.0$, also indicated by a *broken line*; as Fig. 8 shows, for $H = 0$ and finite D, one crosses the line from $T_{trip}^{(D)}$ to $T_c^{(r)}(D)$, and this is the transition located at T_{WD})

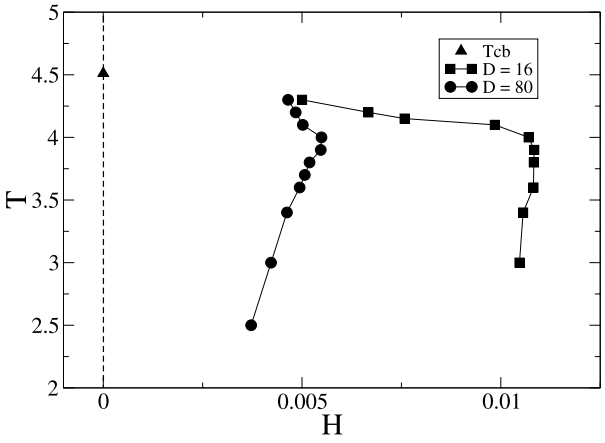

Fig. 11 Plot of the phase diagrams in the T–H plane as obtained for two different film thicknesses. The *filled triangle* at the *vertical dashed line* for $H = 0$ shows the location of the bulk critical temperature. Note that the transition line from $T_{trip}(D)$ to $T_c^{(\ell)}(D)$ is not included here. *Lines* are only drawn to guide the eye

all three first-order transition lines (Fig. 8, lower part) will meet at $T_{trip}(D)$ with nontrivial slopes which are all different from each other.

However, there is no a priori reason to expect that the temperature derivative $dH_c(D, T)/dT > 0$ for $T < T_{trip}(D)$. Since at $T = 0$ the balance between bulk and surface fields simply implies

$$H_c(D, T = 0) = -(H_1 + H_D)/D, \tag{19}$$

i.e. for $H_1 = -0.318$, $H_D = -H_1/2$ yielding $H_c\ (D = 80, T = 0) = 0.001988$, $H_c\ (D = 16, T = 0) = 0.009938$, the phase boundaries shown in Fig. 11 clearly are nicely compatible with their zero temperature limits.

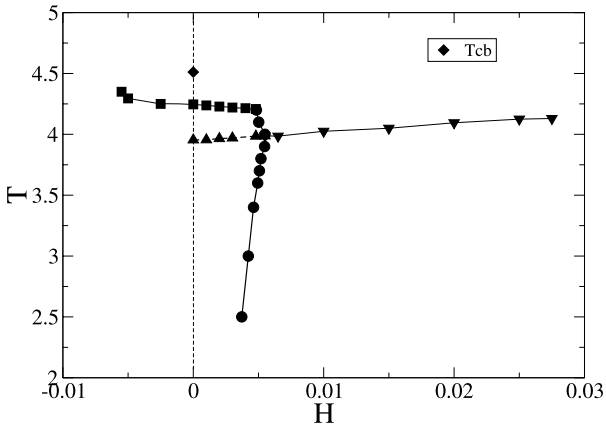

Fig. 12 Phase diagram of a thin Ising film, $D = 80$ layers, plotted in the plane of variables temperature T and bulk field H, and surface fields $H_1 = -0.318$, $H_D = -H_1/2 = 0.159$ (both T, H, and H_1 are measured in units of the exchange constant J). The *circles* represent the transition from negative magnetization (at smaller fields) to positive magnetization (at larger fields) in the regime of temperatures where the right wall (for $D \to \infty$) is nonwet; the *squares* represent the finite film thickness analogue of the prewetting transition of the right wall, the *triangles* pointing down represent the finite film thickness analog of the prewetting transition of the left wall. When this transition line meets the transition line marked by *circles* we reach a thin film triple point. The *triangles* pointing up represent a metastable continuation of the prewetting transition (encountered for metastable states of the film with positive total magnetization). The *diamond* marks the position of the critical point in the bulk

It is also remarkable that the curves for the transition line from $T_{trip}(D)$ to $T_c^{(r)}(D)$ are rather close together for $T = 4.3$ and also have almost the same value of critical field $H_c^{(r)}(D)$. These data hence provide a reasonable first estimate of $T_{c,pre}^{(r)}$ (upper part of Fig. 8). Since the line from $T_{trip}(D)$ to $T_c^{(r)}(D)$ for $D \to \infty$ should develop two distinct parts $T_{trip}(D \to \infty) = T_w^{(\ell)}$, and for $D \to \infty$ the transition occurs at $H = 0$ in the interval $T_w^{(\ell)} < T < T_w^{(r)}$, where then the prewetting line from $T_w^{(r)}$ to $T_{c,pre}^{(r)}$ splits off from the $H = 0$ axis, with $T_c^{(r)}$ $(D \to \infty) = T_{c,pre}^{(r)}$, one expects for finite D a rounded kink in this line near $T = T_W^{(r)}$.

For the thick film ($D = 80$), we have made an attempt to map out the complete phase diagram, and this is shown in Fig. 12. The location of the bulk phase transition between spin-up and spin-down phases (for $D \to \infty$) occurs for $H = 0$, of course (broken line in Fig. 12) and ends at the bulk critical point (shown as a diamond in Fig. 12). For finite D like $= 80$, this transition between spin down phases (left) and spin up phases (right) is shifted towards positive fields $H_c(T)$ in the bulk (circles in Fig. 12), as already shown in Fig. 11. At about $T = 3.9$, this curve has a kink towards left, and there the line of transitions joins which is the analog of prewetting transitions on the left wall for $D \to \infty$. This line is shown by triangles pointing down, in Fig. 12: actually we can follow the metastable continuation of this line (triangles pointing up) for smaller fields down to $H = 0$, since the spin-up phase of the bulk film for fields $0 \le H < H_c(T)$ is sufficiently metastable at $T \le 4.0$ to allow for a precise estimation for the location of this transition. In fact, in this way we are able to estimate that $T_W^{(\ell)} = 3.9 \pm 0.05$ for our model. One should have expected that $T_W^{(\ell)} = 4.0$ for the present system—this slight discrepancy hence is indicative of residual small errors due to finite-size effects and inaccuracies of the numerical integration procedure by which H_1 was chosen in order to have $T_W^{(\ell)} = 4.0$.

The full squares show then the transition line that ends at $T_c^{(r)}(D)$ at a negative field, as expected from the schematic Fig. 8. Note that the kink, which appears for $D \to \infty$ at $T_W^{(r)}$ at $H = 0$, seems still to be visible at about $T \approx 4.2$ (and a nonzero field of about $H \approx 0.004$).

Of course, this kink is sharp only for $D \to \infty$, for large but finite D it is rounded, because it corresponds to a gradual crossover in the character of the phase transition from the bulk spin-up phase → spin-down phase transition to the analog of the prewetting transition at the right wall.

6 Conclusions

In this paper a simulation study of a generic model for the phase behavior of thin Ising films with surface fields of different sign but unequal strength has been carried out. While in the thermodynamic limit ($D \to \infty$) the system would exhibit first-order wetting transitions that occur at different temperatures for the left wall and the right wall, and both wetting transitions as well as the bulk transition occur at the bulk field $H = 0$, in the films with finite thickness D wetting transitions are no longer possible, and the transition where the total magnetization of the film jumps from a negative to a positive value, when H increases, occurs at a nontrivially shifted transition line $H_c(D, T)$. However, the prewetting transition lines that exist for $H \neq 0$ in the limit $D \to \infty$ do have analogs for films of finite thickness. The transition line from $T_W^{(\ell)}$ to $T_{c,pre}^{(\ell)}$ on the left wall of the film, where a strongly negative surface field acts, due to the finite film thickness gets split into a metastable part (for $D \leq H < H_{\rm trip}^{(D)}$) and a stable part (for $H_{\rm trip}^{(\ell)}(D), T_c^{(\ell)}(D)$) is the analog of the prewetting critical point of the left wall (cf. Figs. 8, 12). For large D the location of $(H_c^{(\ell)}(D), T_c^{(\ell)}(D))$ converges rapidly towards $(H_{c,\rm pre}^{(\ell)}, T_{c,\rm pre}^{(\ell)})$ when D increases.

Similarly, the prewetting line of the right wall (which for $D \to \infty$ exists for $H_{c,pre} \leq H \leq 0$ only) becomes essentially part of the line from the thin film critical point $(H_{c,pre}^{(r)}(D), T_c^{(r)}(D))$ to $(H_{\rm trip}(D), T_{\rm trip}(D))$. The existence of the wetting transition at $T_W^{(r)}$, $H = 0$ for $D \to \infty$ for large enough D still leads to a visible (slightly rounded) kink in the curve that connects $T_c^{(r)}(D)$ with $T_{\rm trip}(D)$ (compare Fig. 12 with Fig. 8). The transition from $T_W^{(r)}$ to T_{cb} at $H = 0$, that exists in the limit $D \to \infty$ in spite of the fact that both walls in this region of T are wet, does not have any counterpart in the films of finite thickness, however, irrespective how thick the film is. Thus, our results show that the speculative expectation of how the phase diagram of thin films is related to the bulk phase diagrams is explicitly confirmed by the simulations.

Our results also show that in a thin film a (first-order) wetting transition is observable at conditions where phase coexistence in the bulk occurs for that surface which has the lower wetting transition temperature: since the other surface is then still far from the wetting transition, a metastable nonwet state of the film may occur over wide enough parameter regions to allow the occurrence of wetting phenomena (on the left wall, in our case).

Acknowledgements This work has been supported in part by the Deutsche Forschungsgemeinschaft, Project No SFB 625/A3. E.V.A acknowledged the support of CONICET, ANPCyT, and UNLP (Argentina). We are indebted to Marcus Müller for stimulating discussions during an early stage of this research project. One of us (K.B.) is indebted to E. Brézin for stimulating his interest on wetting phenomena in the Ising model 25 years ago.

References

1. Fisher, M.E., Nakanishi, H.: J. Chem. Phys. **75**, 5857 (1981)

2. Nakanishi, H., Fisher, M.E.: J. Chem. Phys. **78**, 3279 (1983)
3. Evans, R., Taranzona, P.: Phys. Rev. Lett. **52**, 557 (1984)
4. Albano, E.V., Binder, K., Heermann, D.W., Paul, W.: J. Chem. Phys. **91**, 3700 (1989)
5. Albano, E.V., Binder, K., Heermann, D.W., Paul, W.: Surface Sci. **223**, 151 (1989)
6. Nicolaides, D., Evans, R.: Phys. Rev. B **39**, 9336 (1989)
7. Evans, R.: J. Phys., Condens. Matter **2**, 8989 (1990)
8. Parry, A.O., Evans, R.: Phys. Rev. Lett. **64**, 439 (1990)
9. Parry, A.O., Evans, R.: Physica A **181**, 250 (1992)
10. Binder, K., Landau, D.P.: J. Chem. Phys. **96**, 1444 (1992)
11. Binder, K., Landau, D.P., Ferrenberg, A.M.: Phys. Rev. E **51**, 2823 (1995)
12. Binder, K., Evans, R., Landau, D.P., Ferrenberg, A.M.: Phys. Rev. E **53**, 5023 (1996)
13. Ferrenberg, A.M., Landau, D.P., Binder, K.: Phys. Rev. E **58**, 3353 (1998)
14. Gelb, L.D., Gubbins, K.E., Radhakrishnan, R., Sliwinska-Bartkowiak, M.: Rep. Prog. Phys. **62**, 1573 (1999)
15. Müller, M., Binder, K., Albano, E.V.: Physica A **279**, 188 (2000)
16. Müller, M., Albano, E.V., Binder, K.: Phys. Rev. E **62**, 5281 (2000)
17. Müller, M., Binder, K., Albano, E.V.: Europhys. Lett. **49**, 724 (2000)
18. Müller, M., Binder, K.: Phys. Rev. E **63**, 021602 (2001)
19. Dillmann, O., Janke, W., Müller, M., Binder, K.: J. Chem. Phys. **114**, 5853 (2001)
20. Binder, K., Landau, D.P., Müller, M.: J. Stat. Phys. **110**, 1411 (2003)
21. Schmidt, M., Fortini, A., Dijkstra, M.: J. Phys., Condens. Matter **1553**, S3411 (2003)
22. Schmidt, M., Fortini, A., Dijkstra, M.: J. Phys., Condens. Matter **16**, S4159 (2004)
23. Schulz, B.J., Binder, K., Müller, M.: Phys. Rev. E **71**, 046705 (2005)
24. Vink, R.L.C., Binder, K., Horbach, R.: Phys. Rev. E **73**, 056118 (2006)
25. Vink, R.L.C., de Virgiliis, A., Horbach, J., Binder, K.: Phys. Rev. E **74**, 031601 (2006)
26. de Virgiliis, A., Vink, R.L.C., Horbach, J., Binder, K.: Eur. Phys. Lett. **77**, 60002 (2007)
27. Binder, K., Horbach, J., Vink, R.L.C., de Virgiliis, A.: Soft Matter **4**, 1555 (2008)
28. Ising, E.: Z. Phys. **31**, 253 (1925)
29. Chowdbury, D., Stauffer, D.: Principles of Equilibrium Statistical Mechanics. Wiley-VCH, Weinheim (2000)
30. Binder, K., Hohenberg, P.C.: Phys. Rev. B **6**, 3461 (1972)
31. Binder, K., Hohenberg, P.C.: Phys. Rev. B **9**, 2194 (1974)
32. Kerle, T., Klein, J., Binder, K.: Phys. Rev. Lett. **77**, 1318 (1996)
33. Kerle, T., Klein, J., Binder, K.: Eur. Phys. J. B **7**, 401 (1999)
34. Decker, G., Schlenoff, J.B. (eds.): Multilayer Thin Films: Sequential Assembly of Nanocomposite Materials. Wiley-VCH, Weinheim (2002)
35. Champion, Y., Fecht, H.J. (ed.): Nano-Architectured and Nano-Structured Materials. Wiley-VCH, Weinheim (2004)
36. Kelsall, R., Hamley, I.W., Geohegan, M. (eds.): Nanoscale Science and Technology. Wiley-VCH, Weinheim (2005)
37. Binder, K., Landau, D.P.: Phys. Rev. B **37**, 1745 (1988)
38. Binder, K., Landau, D.P., Wansleben, S.: Phys. Rev. B **40**, 6971 (1989)
39. Binder, K., Landau, D.P.: Phys. Rev. B **46**, 4844 (1992)
40. de Gennes, P.G.: Rev. Mod. Phys. **57**, 825 (1985)
41. Sullivan, D.E., Telo da Gama, M.M.: In: Croxton, C.A. (ed.) Fluid Interfacial Phenomena, p. 45. Wiley, New York (1986)
42. Dietrich, S.: In: Domb, C., Lebowitz, J.L. (eds.) Phase Transitions and Critical Phenomena, vol. XII, p. 1. Academic Press, New York (1988)
43. Bonn, D., Ross, D.: Rep. Prog. Phys. **64**, 1085 (2001)
44. Brézin, E., Halperin, B.I., Leibler, S.: Phys. Rev. Lett. **50**, 1387 (1983)
45. Parry, A.O., Rascon, C., Bernardino, N.R., Romero-Enrique, J.M.: Phys. Rev. Lett. **100**, 136105 (2008) and to be published
46. Ferrenberg, A.M., Landau, D.P.: Phys. Rev. B **44**, 5081 (1991)
47. Landau, D.P., Binder, K.: A Guide to Monte Carlo Simulation in Statistical Physics, 2nd edn. Cambridge University Press, Cambridge (2005)
48. Swendsen, R.H., Wang, J.-S.: Phys. Rev. Lett. **58**, 86 (1987)
49. Wolff, U.: Phys. Rev. Lett. **62**, 361 (1989)
50. Wang, F., Landau, D.P.: Phys. Rev. Lett. **86**, 2050 (2001)
51. Wang, F., Landau, D.P.: Phys. Rev. E **64**, 056101 (2001)
52. Neuhaus, T., Hager, J.S.: J. Stat. Phys. **113**, 47 (2003)
53. Binder, K., Landau, D.P.: Phys. Rev. B **30**, 1477 (1984)

54. Challa, M.S.S., Landau, D.P., Binder, K.: Phys. Rev. B **34**, 1841 (1986)
55. Borgs, C., Kotecky, R.: J. Stat. Phys. **61**, 79 (1990)
56. Privman, V. (ed.): Finite Size Scaling and Numerical Simulation of Statistical Systems. World Scientific, Singapore (1990)
57. Binder, K.: Z. Phys. B **45**, 61 (1981)
58. Binder, K.: In: Domb, C., Lebowitz, J.L. (eds.) Phase Transitions and Critical Phenomena, vol. 8, p. 1. Academic Press, New York (1983)
59. Hasenbusch, M., Pinn, K.: Physica A **192**, 343 (1993)
60. Hasenbusch, M., Pinn, K.: Physica A **203**, 189 (1994)
61. Müller, M., Binder, K.: Macromolecules **31**, 8323 (1998)